Performance Analysis of Dual-Hop RF/FSO Relaying Systems with Imperfect CSI

Zihan Zhang, Qiang Sun, Miguel López-Benítez, Xiaomin Chen, and Jiayi Zhang, *Senior Member, IEEE*

***Abstract*—This paper proposes a unified performance analysis framework of asymmetric dual-hop radio-frequency/free-space optical (RF/FSO) transmission systems. The generalized independent and identically distributed (i.i.d.) $\alpha-\mu$ distribution is considered for each branch in the RF link, whereas the FSO link is assumed to experience Málaga ($\mathcal{M}$) fading with pointing error impairments. With amplify-and-forward (AF) and decode-and-forward (DF) relaying, the imperfect channel state information (CSI) of both links is considered. For the considered system, we first derive exact and novel analytical expressions for the probability density function (PDF) and cumulative distribution function (CDF) of the end-to-end signal-to-noise ratio (SNR). Furthermore, we obtain key performance metrics such as outage probability (OP), average bit-error-rate (ABER), and effective capacity (EC). The important effects of channel parameters on the system are disclosed from mathematical analysis and are further validated by Monte-Carlo simulations.**

***Index Terms*—performance analysis, Free space optical communication, $\alpha-\mu$ distribution, Málaga ($\mathcal{M}$) fading, imperfect CSI.**

I. Introduction

The increasing amount of connected nodes and the occurrence and growth of high-volume services have a significant effect on the new generation of wireless communication networks. Proximity-based communication systems, such as device-to-device wireless networks and their byproducts, have opened their doors in these ultra-dense networks [1]. The communication burdens have shifted from the core to the access interface in data traffic networks supporting these services. The fifth-generation (5G) technology standard is required to offer services including low latency, massive throughput, and high-speed network [2]. To accomplish this high demand is certainly a huge challenge [3]. Free space optical (FSO) technology requires no license fees because it relies on laser beams at frequencies above 300 GHz. Compared with the radio frequency (RF) communication, there are several outstanding virtues of the FSO system, such as high safety, low persistence, lower power depletion ($\sim$1/2 of RF), smaller dimensions ($\sim$1/10 of the RF antenna size), and easy installation without optical fiber deployment [4]. These advantages make of FSO systems an excellent replacement for conventional RF systems. However, the FSO system performance is limited by practical impairments such as atmospheric turbulence (e.g., dust, fog, clouds, and snow,) and pointing errors [5]. As a useful technology, relaying has been generally made use of in practical telecommunication networks [6]. To solve the afore-mentioned issues, hybrid FSO/RF systems have attracted much attention from academia and industry. Hybrid RF/FSO systems merge the best features of both technologies and, when combined with relaying techniques, can enhance the system performance significantly.

Z. Zhang, Q. Sun, X. Chen and J. Zhang are with the School of Information Science and Technology, Nantong University, Nantong 226019, China. (e-mail: sunqiang@ntu.edu.cn).

M. López-Benítez is with the Department of Electrical Engineering and Electronics, University of Liverpool, Liverpool, L69 3GJ, United Kingdom, and also with the ARIES Research Centre, Antonio de Nebrija University, 28040 Madrid, Spain (e-mail: m.lopez-benitez@liverpool.ac.uk).

A. Related Work

In [7], Lee et al. have analyzed the performance of the asymmetric RF/FSO relay system. The performance analysis has been further studied on mixed RF/FSO relay systems over several fading channels [8]–[18]. In most of existing works on hybrid RF/FSO systems, the FSO link is assumed to undergo Gamma-Gamma turbulence [10]–[12], [18], the double generalized Gamma distribution [8], [9], the M-distributed fading [13], the mixture Exponential-Generalized Gamma distribution [14], the Exponentiated Weibull fading channel [15], the Generalized Málaga distribution [16], and Málaga ($\mathcal{M}$) distribution [17], respectively. For the RF link, Nakagami-m and/or Generalized Nakagami-m distributions are generally modeled [8], [11], [12], [15], [16], [19], Rayleigh fading [13], [18], [20], as well as $\kappa-\mu$, $\eta-\mu$, the extended generalized-K shadowed fading, Generalized-K distribution, $\alpha-\mu$ fading and Fisher-Snedecor F fading models, see e.g., in [10], [17], [9], [14]. Nevertheless, these works were carried out under the assumption that perfect CSI was obtainable. In practice, it is impractical to get perfect CSI for wireless channels due to channel estimation errors and feedback errors [21]. Performance analysis of the RF/FSO dual-hop link was presented in [22] with imperfect CSI, Rayleigh faded MIMO channel for the RF link and Gamma-Gamma fading for the FSO link. The authors of [23] studied the performance of multiuser mixed RF/FSO relay networks with generalized order user scheduling considering the outdated CSI. Even though the above works in [22], [23] are insightful, these results assume a Rayleigh fading channel model which models a homogeneous scattering condition. In reality, since the received signals are spatially correlated, a nonlinear function of the modulus of the sum of the multipath components can more accurately model the nonhomogeneous scattering environment [24], [25]. In this paper, we deal with the above issues by analyzing the performance of dual-hop asymmetrical RF/FSO systems. Note that under both heterodyne detection and intensity modulation with direct detection (IM/DD) methods, the FSO link considers the pointing error impairment. The

FSO system can be installed with boresight error[1] close to zero or even negligible when the transmitter and receiver in the single-input-single-output FSO link are properly aligned [26], [27]. To the best of the author's knowledge, only the studies [28] and [29] consider the imperfect CSI in RF and FSO channels of the RF/FSO systems. However, they all focus on the secrecy performance. In this work, we fill this gap by offering a general analytical framework of the considered systems with imperfect CSI. Also, we provided the novel closed-form expressions for various performance metrics such as the OP, BER, and EC. Designing practical RF/FSO systems with imperfect CSI, these novel results can provide significant insights. Specifically, the EC considers the delay limitations imposed by emerging real-time applications with various quality of service (QoS) demands [5]. the relay equips with multiple antennas, based on maximal-ratio combining (MRC) to enhance the received signal-to-noise ratio (SNR). In addition, we investigate more realistic scenarios where the RF and FSO links are both considered imperfect CSI, which are modeled by the sum of generalized independent identically distributed (i.i.d.)[2] $\alpha-\mu$ and Málaga ($\mathcal{M}$) fading. Furthermore, $\alpha-\mu$ fading has some outstanding qualities, for instance universality, adaptability, and arithmetical manageability. The $\alpha-\mu$ fading includes other distributions such as Rayleigh, Nakagami-m, Negative Exponential, One-Sided Gaussian, and Weibull [30] as special cases. Moreover, The non-linearity of the physical channel can be expressed by this fading model. These advantageous characteristics of $\alpha-\mu$ fading make it an appropriate candidate to be used in the RF link. Furthermore, Málaga ($\mathcal{M}$) fading integrates most fading models for the FSO link, including both lognormal and Gamma-Gamma models as special cases, and can describe a more extensive reflection of turbulence conditions [31]. The contributions of this work can be summarized as follows:

1) We propose an asymmetrical RF/FSO relay system model for wireless communications in which $\alpha-\mu$ fading and Málaga ($\mathcal{M}$) fading are considered. Operating both AF and DF relaying, the FSO link experiences both effect of atmosphere turbulence and pointing error. Capitalizing on the effect of imperfect CSI, a novel and exact closed-form CDF expression for the end-to-end SNR is derived.
2) Significant theoretical and practical insights are provided by investigating the effects of the imperfect CSI and channel parameters on the system performance.
3) Due to the difficulty to obtain exact closed-form expressions, and in order to analyze the influence of each parameter on the performance, we provide the asymptotic propertes of the derived OP of the DF scheme at the high SNR regime in terms of simple elementary functions.

[1]The analysis of the effect of non-zero boresight pointing errors will be conducted in our future work based on the results of this paper.

[2]The generalization of this work to non-i.i.d. fading channels is promising for future research.

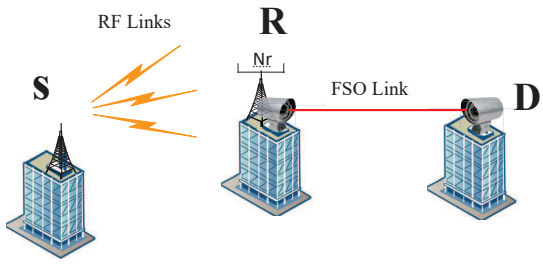

Fig. 1. Mixed RF/FSO communication system model.

B. Organization

The remainder of the paper is organized as follows. Section II presents the channel and system models. The statistical features of the end-to-end SNR of the considered system are presented in Section III. The performance metrics such as outage probability, average bit error rate, and effective capacity are derived in Section IV. Section V supplies Monte Carlo and analytical results. Finally, Section VI concludes the paper.

II. System Model

We consider a dual-hop asymmetric RF/FSO system depicted in Fig. 1, which has an FSO receiver (D) and an RF transmitter (S), each equipped with a single antenna. The relay (R) has N_r antennas and only a photo-diaphragm sending set on the optical side. The system works on the principle of the MRC diversity using both AF and DF relays. Due to obstacles, the link between the transmitter and the receiver has no direct line-of-sight. The RF links and the FSO link experience $\alpha-\mu$ fading and Málaga ($\mathcal{M}$) fading, respectively, wherein the CSI is imperpect.

A. RF Link

Using MRC, the channel gain of the RF links can be expressed as

$$|h_{\mathrm{RF,s}}|^2 = \sum_{i=1}^{N_r} |h_{\mathrm{RF,i}}|^2, \tag{1}$$

where $h_{\mathrm{RF,i}}$ represents the channel coefficient of RF link between transmitter and relay's N_{r} antennas, which is assumed to undergo $\alpha-\mu$ fading. The received signal at R can be written as [32, Eq. (2)]

$$y_R(i) = \hat{h}_{\mathrm{RF,s}} x(i) + n_{\mathrm{SR}}, \tag{2}$$

where n_{SR} is the additive white Gaussian noise (AWGN) with variance σ_n^2. The message block can be encoded at the transmitter in terms of the codeword $x^{N_r} =$

TABLE I
LITERATURE ON MIXED RF/FSO SYSTEMS

Ref.	RF Link	FSO Link	CSI	Performance Metrics
[7]	Rayleigh	Gamma-Gamma	Perfect	OP
[8]	Nakagami-m	Double generalized gamma	Perfect	OP, BER
[9]	extended generalized-$K(EGK)$	double generalized Gamma (DGG)	Perfect	OP, BER, Ergodic Capacity
[10]	Generalized $\kappa-\mu$ or $\eta-\mu$	Gamma-Gamma	Perfect	OP, BER
[11]	Nakagami-m	Gamma-Gamma	Perfect	OP, BER
[12]	the generalized Nakagami-m	Gamma-Gamma	Perfect	OP, BER
[13]	Rayleigh	M-distributed	Perfect	OP
[14]	Generalized-K	Mixture Exponential-Generalized Gamma	Perfect	OP, BER, Average Channel Capacity
[15]	Nakagami-m	Exponentiated Weibull	Perfect	OP, BER
[16]	Nakagami-m	Generalized Málaga	Perfect	OP,BER, Ergodic Capacity
[17]	$\kappa-\mu$	Málaga-$\mathcal{M}$	Perfect	OP, Ergodic Capacity
[18]	Rayleigh	Gamma-Gamma	Perfect	OP, BER
[19]	the generalized Nakagami-m	Gamma-Gamma	Imperfect	OP, BER, Ergodic Capacity
[23]	Rayleigh	Gamma-Gamma	Outdated	OP, BER, Ergodic Capacity
[28]	Rayleigh	Gamma-Gamma	Imperfect	SOP
[29]	Nakagami-m	Málaga	Outdated and Imperfect	The effective secrecy throughput
Our Work	$\alpha-\mu$	Málaga ($\mathcal{M}$)	Imperfect	OP, BER, Effective Capacity

$[x(1), x(2), ...x(i)..., x(N_r)]$, which is appropriate to communicate through the $\alpha-\mu$ fading channel. $\hat{h}_{\text{RF,i}}$ represents the estimated RF channel gain which can be written as [33, Eq. (3)]

$$\hat{h}_{\text{RF,i}} = \rho_{\text{RF}} h_{\text{RF,i}} + \sqrt{1-\rho_{\text{RF}}^2}\varepsilon, \tag{3}$$

where $\rho_{\text{RF}} \in (0,1]$ is a constant denoting the CSI accurateness. The CSI estimation error decreases as the value of ρ_{RF} increases, and $\rho_{\text{RF}} = 1$ means that there is no CSI estimation error. The instantaneous SNR of the imperfect RF link $\hat{\gamma}_{\text{RF}}$ can be written as

$$\hat{\gamma}_{\text{RF}} = R^2 E_{\text{s}}/N_0 = \bar{\gamma}_{\text{RF}} \hat{h}_{\text{RF,s}}^2, \tag{4}$$

where R denotes the envelopes of the received signals, and $\bar{\gamma}_{\text{RF}}$ is the average SNR. N_0 and E_{s} represent the single-sided noise power spectral density and the average symbol energy, respectively.

Lemma 1: The PDF and CDF of $\hat{\gamma}_{\text{RF}}$ are given as

$$f_{\hat{\gamma}_{\text{RF}}}(\gamma) = \begin{cases} \sum_{k=0}^{\infty} C_2 \varphi^{\frac{k+1}{2}} \gamma^{\frac{k-1}{2}} \exp(-\varphi\gamma) & \gamma > 0 \\ 1 - Z_1 & \gamma = 0 \end{cases} \tag{5}$$

$$F_{\hat{\gamma}_{\text{RF}}}(\gamma) = \begin{cases} \sum_{k=0}^{\infty} C_2 G_{1,2}^{1,1}\left[\varphi\gamma \,\middle|\, \begin{matrix} 1 \\ \frac{1+k}{2}, 0 \end{matrix}\right] & \gamma > 0 \\ 1 - Z_1 & \gamma = 0 \end{cases} \tag{6}$$

where $C_2 \triangleq \frac{\alpha 2^{k-2} G_k}{k!\sqrt{\pi}\Gamma(\mu)}$, $\varphi \triangleq \frac{1}{2N_r^2 \bar{\gamma}_{\text{RF}}\left(1-\rho_{\text{RF}}^2\right)}$, $Z_1 \triangleq \sum_{k=0}^{\infty} \frac{\alpha\Gamma(\frac{1+k}{2}) 2^{k-2} G_k}{k!\sqrt{\pi}\Gamma(\mu)}$, μ and α are two physical parameters, which represent the number of multipath clusters and the non-linearity of the environment, respectively. $G_{p,q}^{m,n}[\cdot]$ [34, Eq. (9.301)] and $\Gamma(\cdot)$ [34, Eq. (8.310)] denotes the Meijer's G-function and the Gamma functions, respectively. $G_k = H_{1,1}^{1,1}\left[\frac{\mu(2(1-\rho_{\text{RF}}{}^2)N_r{}^2)^{\frac{\alpha}{2}}}{(\rho_{\text{RF}}\hat{r})^{\alpha}} \,\middle|\, \begin{matrix} (1-\frac{k}{2}, \frac{\alpha}{2}) \\ (\mu, 1) \end{matrix}\right]$, in which $H_{p,q}^{m,n}[\cdot]$ [35, Eq. (1.1.1)] denotes the the Fox's H-function.

Proof: Please see Appendix A. ■

B. FSO Link

The probability density function (PDF) and the cumulative distribution function (CDF) of the FSO link SNR $\hat{\gamma}_{\text{FSO}}$ are given by [28, Eq. (3), Eq. (4)]

$$f_{\hat{\gamma}_{\text{FSO}}}(\gamma) = \begin{cases} B_1 \sum_{h=1}^{\beta} \sum_{i=0}^{\infty} b_h \varphi_1 \gamma^{\frac{i+1}{r}-1} e^{-\psi_1 \gamma^{\frac{2}{r}}} & \gamma > 0 \\ 1 - Z & \gamma = 0 \end{cases} \tag{7}$$

$$F_{\hat{\gamma}_{\text{FSO}}}(\gamma) = \begin{cases} B_1 \sum_{h=1}^{\beta} \sum_{i=0}^{\infty} H_1 G_{1,2}^{1,1}\left[\psi_1 \gamma^{\frac{2}{r}} \,\middle|\, \begin{matrix} 1 \\ \frac{1+i}{2}, 0 \end{matrix}\right] & \gamma > 0 \\ 1 - Z & \gamma = 0 \end{cases} \tag{8}$$

where the type of detection technique is defined by the parameter r. $r = \{1, 2\}$ denotes heterodyne and IM/DD detection, respectively. The value of a and β show the severity level of atmospheric turbulence. The off-axis eddies receive the average power of the scattering component which can be represented as $g = 2b_0(1-\rho_0)$, with ρ_0 denoting the number of scattering power coupled to the line-of-sight (LOS) component, and the average power of the total scatter components $2b_0$. $B_1 \triangleq \frac{2^{a-4.5} A_1 \xi^2}{\pi^{1.5}}$, $A_1 \triangleq \frac{2a^{0.5a}\left(\frac{\beta g}{\beta g+\Omega_1}\right)^{0.5a+\beta}}{\Gamma(a) g^{1+0.5a}}$, $b_h \triangleq \frac{(\beta-1)! a^{0.5h} \Omega_1^{h-1} (\beta g+\Omega_1)^{1-0.5h}}{g^{h-1}\beta^{0.5h}((h-1)!)^2(\beta-h!)}\left(\frac{\beta a}{\beta g+\Omega_1}\right)^{-0.5(h+a)}$, $\psi_1 \triangleq \frac{1}{2\overline{\gamma}_{\text{FSO}}^{\frac{2}{r}}\left(1-\rho_{\text{FSO}}^2\right)}$, $\varphi_1 \triangleq \frac{G_i 2^{h+0.5i}}{i! r (1-\rho_{\text{FSO}}^2)^{0.5(i+1)} \overline{\gamma}_{\text{FSO}}^{\frac{1+i}{r}}}$, $H_1 \triangleq \frac{2^{i+h-0.5} b_h G_i}{i!}$, $Z \triangleq \frac{A_1 \xi^2}{\pi^{1.5}} \sum_{h=1}^{\beta} \sum_{i=0}^{\infty} \Gamma\left(\frac{1+i}{2}\right) \frac{2^{i+a+h-5} G_i b_h}{i!}$. $\Omega_1 \triangleq 2\rho_0 b_0 + \Omega + 2\sqrt{2\rho_0 b_0 \Omega}\cos(\varphi_A - \varphi_B)$ is the average power of the coherent contributions, where Ω is the average power of the LOS component, φ_{A} and φ_{B} are the deterministic phases of the LOS and the coupled-to-LOS scatter terms, respectively. $G_i = G_{6,3}^{1,6}\left[\frac{2^3}{\delta^2(1-\rho_{\text{FSO}}{}^2)} \,\middle|\, \begin{matrix} \frac{1-\xi^2}{2}, \frac{2-\xi^2}{2}, \frac{1-a}{2}, \frac{2-a}{2}, \frac{1-h}{2}, \frac{2-h}{2} \\ \frac{i}{2}, -\frac{\xi^2}{2}, \frac{1-\xi^2}{2} \end{matrix}\right]$, where $\delta \triangleq \frac{a\beta}{A_0 I_l \rho_{\text{FSO}}(\Omega_1+\beta g)}$. I_l is a constant in a given weather condition that represents the path loss. A_0 and ξ are constant terms that determine the pointing loss ($\xi \to \infty$

means negligible pointing errors).

III. Statistics of End-To-End SNR

A. AF Relay with Fixed-Gain

Proposition 1. *Supposing a fixed gain relay, the end-to-end SNR can be calculated as* $\hat{\gamma}^{AF} = \frac{\hat{\gamma}_{\rm FSO}\hat{\gamma}_{\rm RF}}{\hat{\gamma}_{\rm RF}+C_R}$ *[36], where* $\hat{\gamma}_{FSO}$ *and* $\hat{\gamma}_{RF}$ *are FSO and RF links instantaneous SNRs, respectively.* C_R *represents a parameter associated with the fixed relay gain. The CDF for the considered system can be derived in closed-form as*

$$\begin{aligned} F_{AF}(\gamma) &= 1 - B_1 \sum_{\rm h=1}^{\beta}\sum_{k=0}^{\infty} H_1 G_{1,2}^{2,0}\left[\frac{\gamma^2}{2\left(1-\rho_{FSO}^2\right)}\middle|\begin{matrix}1\\ \frac{1+i}{2},0\end{matrix}\right] \\ &+ \sum_{\rm h=1}^{\beta}\sum_{k=0}^{\infty}\sum_{i=0}^{\infty} b_h\varphi_1 C_2 B_1 \gamma^{\frac{1+i}{r}} H_{1,0:1,3:1,1}^{0,1:2,1:0,1} \\ &\left[\begin{matrix}\left(1+\frac{1+i}{r};1,\frac{2}{r}\right)\\ - \\ (1,1)\\ (1,1)\left(\frac{1+k}{2},1\right)(0,1)\\ (1,1)\\ \left(\frac{1+i}{r},\frac{2}{r}\right)\end{matrix}\middle|\begin{matrix}\\ \\ \\ \varphi C_R,\left(\frac{1}{\psi_1\gamma}\right)^{\frac{2}{r}}\\ \\ \\ \end{matrix}\right], \end{aligned} \tag{9}$$

where $H_{p1,q1:p2,q2:p3,q3}^{0,n1:m2,n2:m3,n3}[\cdot]$ refers to the bivariate Fox's-H function [37].

Proof: Please see Appendix B. ■

Truncating (10) to the first N_1 and N_2 terms, we can get

$$\begin{aligned} \widetilde{F}_{\rm AF}(\gamma) &= 1 - B_1 \sum_{\rm h=1}^{\beta}\sum_{k=0}^{N_1} H_1 G_{1,2}^{2,0}\left[\frac{\gamma^2}{2\left(1-\rho_{\rm FSO}^2\right)}\middle|\begin{matrix}1\\ \frac{1+i}{2},0\end{matrix}\right] \\ &+ \sum_{\rm h=1}^{\beta}\sum_{k=0}^{N_1}\sum_{i=0}^{N_2} b_h\varphi_1 C_2 B_1 \gamma^{\frac{1+i}{r}} H_{1,0:1,3:1,1}^{0,1:2,1:0,1} \\ &\left[\begin{matrix}\left(1+\frac{1+i}{r};1,\frac{2}{r}\right)\\ - \\ (1,1)\\ (1,1)\left(\frac{1+k}{2},1\right)(0,1)\\ (1,1)\\ \left(\frac{1+i}{r},\frac{2}{r}\right)\end{matrix}\middle|\begin{matrix}\\ \\ \\ \varphi C_R,\left(\frac{1}{\psi_1\gamma}\right)^{\frac{2}{r}}\\ \\ \\ \end{matrix}\right], \end{aligned} \tag{10}$$

The truncation error of $\widetilde{F}_{AF}(\gamma)$ relative to the previous N_1 and N_2 terms is given by

$$\varepsilon(N_1,N_2) = F_{AF}(\infty) - \widetilde{F}_{AF}(\infty) \tag{11}$$

TABLE II
Required terms N_1 and N_2 for the truncation error ($\varepsilon < 10^{-5}$) with different parameters a, β, and ξ.

System and channel parameters	N_1	N_2	ε
$a=2.296, \beta=2, \xi=1.1$	7	17	9.38997×10^{-6}
$a=4.2, \beta=3, \xi=1.1$	7	19	8.78283×10^{-6}
$a=2.296, \beta=2, \xi=6.7$	7	27	9.55683×10^{-6}
$a=4.2, \beta=3, \xi=6.7$	7	35	9.35421×10^{-6}

The convergency of the series in (10) can be proved by Table II, which indicates the required terms N_1 and N_2 for different channel parameters. Notice that N_1 only needs less than 10 terms, and N_2 needs less than 40 terms to achieve a satisfying accurateness (e.g., smaller than 10^{-5}).

B. DF Relaying

Proposition 2. *Based on the end-to-end SNR of a DF relayed system* $\hat{\gamma}^{DF} = \min(\hat{\gamma}_{\rm FSO}, \hat{\gamma}_{\rm RF})$ *[9, Eq. (26)]. Noting that the links suffer fading independently, the CDF at the destination can be formulated as*

$$\begin{aligned} &F_{\hat{\gamma}^{DF}}(\gamma) = F_{\hat{\gamma}_{\rm RF}}(\gamma) + F_{\hat{\gamma}_{\rm FSO}}(\gamma) - F_{\hat{\gamma}_{\rm RF}}(\gamma) F_{\hat{\gamma}_{\rm FSO}}(\gamma) \\ &= 1 - F_{\hat{\gamma}_{\rm RF}}^{C}(\gamma) F_{\hat{\gamma}_{\rm FSO}}^{C}(\gamma), \end{aligned} \tag{12}$$

where $F_{\gamma}^{C}(\cdot)$ *is the complementary CDF (CCDF) of* γ.

Proof: By substituting (8) *and* (6)*, then the CDF can be written as in* (13) *after some manipulations. Thus, the proof is completed.* ■

$$\begin{aligned} F_{\hat{\gamma}^{DF}}(\gamma) &= 1 - \left(Z_1 - F_{\hat{\gamma}_{\rm RF}}(\gamma)\right)\left(Z - F_{\hat{\gamma}_{\rm FSO}}(\gamma)\right) \\ &= 1 - \left(Z1 - C_2\sum_{k=0}^{\infty} G_{1,2}^{1,1}\left[\varphi\gamma\middle|\begin{matrix}1\\ \frac{1+k}{2},0\end{matrix}\right]\right) \\ &\times \left(Z - B_1\sum_{h=1}^{\beta}\sum_{i=0}^{\infty} H_1 G_{1,2}^{1,1}\left[\psi_1\gamma^{\frac{2}{r}}\middle|\begin{matrix}1\\ \frac{1+i}{2},0\end{matrix}\right]\right) \end{aligned}. \tag{13}$$

By utilising [35, Eq. (1.59)] and at high-SNRs, (13) can be rewritten by

$$F_{\hat{\gamma}^{DF}}^{\infty}(\gamma) = F_{\hat{\gamma}_{\rm FSO}}^{\infty}(\gamma) + F_{\hat{\gamma}_{\rm RF}}^{\infty}(\gamma) - F_{\hat{\gamma}_{\rm FSO}}^{\infty}(\gamma) F_{\hat{\gamma}_{\rm RF}}^{\infty}(\gamma), \tag{14}$$

where

$$F_{\hat{\gamma}_{\rm FSO}}^{\infty}(\gamma) = \begin{cases} B_1\sum_{h=1}^{\beta}\sum_{i=0}^{\infty} H_1 \frac{2}{1+i}(\psi_1\gamma^{\frac{2}{r}})^{\frac{1+i}{2}} & \gamma > 0 \\ 1 - Z & \gamma = 0 \end{cases}, \tag{15}$$

$$F_{\hat{\gamma}_{\rm RF}}^{\infty}(\gamma) = \begin{cases} \sum_{k=0}^{\infty} \frac{2C_2}{1+k}(\varphi\gamma)^{\frac{1+k}{2}} & \gamma > 0 \\ 1 - Z_1 & \gamma = 0 \end{cases}. \tag{16}$$

The diversity gain G_d decides the slope of the OP versus average SNR curve. The coding gain G_c decides the shift of the curve in SNR relative to a benchmark OP curve of $(\bar{\gamma})^{-G_d}$. The diversity gain and the coding gain can be written as [38]

$$P_{out} \approx (G_c \cdot \bar{\gamma})^{-G_d}. \tag{17}$$

Assuming perfect CSI, the OP can be parameterized with

$$G_d = \min\left(\frac{1}{r}, \frac{1}{2}\right), \tag{18}$$

and

$$G_c = \begin{cases} 8\pi(1-{\rho_{RF}}^2)\left(\frac{N_r\Gamma(\mu)}{\alpha G_{k_0}}\right)^2 \\ +\left(B_1\sum_{h=1}^{\beta} 2^{h+0.5} b_h G_{i_0}\right)^{-2}\left(\frac{2(1-{\rho_{FSO}}^2)}{\gamma_{th}}\right), & \frac{1}{r}=\frac{1}{2} \\ 8\pi(1-{\rho_{RF}}^2)\left(\frac{N_r\Gamma(\mu)}{\alpha G_{k_0}}\right)^2, & \frac{1}{r}>\frac{1}{2} \end{cases} \tag{19}$$

where $G_{k_0} = H_{1,1}^{1,1}\left[\frac{\mu(2(1-{\rho_{RF}}^2){N_r}^2)^{\frac{\alpha}{2}}}{(\rho_{RF}\hat{r})^{\alpha}}\middle|\begin{matrix}(1,\frac{\alpha}{2})\\ (\mu,1)\end{matrix}\right]$, and $G_{i_0} =$

$G_{6,3}^{1,6}\left[\frac{2^3}{\delta^2(1-\rho_{FSO^2})}\middle|\begin{matrix}\frac{1-\xi^2}{2},\frac{2-\xi^2}{2},\frac{1-\alpha}{2},\frac{2-\alpha}{2},\frac{1-h}{2},\frac{2-h}{2}\\0,-\frac{\xi^2}{2},\frac{1-\xi^2}{2}\end{matrix}\right]$. Truncating (15) and (16) to the first N_3 and N_4 terms, we can get

$$\widetilde{F}_{\hat{\gamma}_{\text{FSO}}^{\infty}}(\gamma)=\begin{cases}B_1\sum\limits_{h=1}^{\beta}\sum\limits_{i=0}^{N_3}H_1\frac{2}{1+i}(\psi_1\gamma^{\frac{2}{r}})^{\frac{1+i}{2}} & \gamma>0\\ 1-Z & \gamma=0\end{cases}, \quad (20)$$

$$\widetilde{F}_{\hat{\gamma}_{\text{RF}}^{\infty}}(\gamma)=\begin{cases}\sum\limits_{k=0}^{N_4}\frac{2C_2}{1+k}(\varphi\gamma)^{\frac{1+k}{2}} & \gamma>0\\ 1-Z_1 & \gamma=0\end{cases}. \quad (21)$$

From the diversity gain and coding gain, we can see that the slope of the performance curve is only related to the type of detection technique at high SNR. The shift of the performance curve relative to a benchmark curve is decided by both system and channel parameters.

The truncation error of $\widetilde{F}_{\hat{\gamma}^{DF}}^{\infty}(\gamma)$ and $\widetilde{F}_{\hat{\gamma}_{\text{FSO}}}^{\infty}(\gamma)$ relative to the N_3 terms and N_4 terms are respectively given by

$$\varepsilon_1(N_3)=F_{\hat{\gamma}_{\text{FSO}}}^{\infty}(\infty)-\widetilde{F}_{\hat{\gamma}_{\text{FSO}}}^{\infty}(\infty) \quad (22)$$

$$\varepsilon_2(N_4)=F_{\hat{\gamma}_{\text{RF}}}^{\infty}(\gamma)-\widetilde{F}_{\hat{\gamma}_{\text{RF}}}^{\infty}(\gamma) \quad (23)$$

TABLE III
REQUIRED TERMS N_3 FOR THE TRUNCATION ERROR ($\varepsilon_1<10^{-13}$) WITH DIFFERENT PARAMETERS ρ.

The CSI accurateness parameters	N_3	ε_1
$\rho=0.5$	4	2.20102×10^{-14}
$\rho=0.9$	5	1.08247×10^{-15}
$\rho=0.95$	6	1.11022×10^{-16}

Table III shows the convergence of the infinite series in (15) by presenting the required truncation terms N_3 for different parameters. Note that only less than 10 terms are needed for the series to converge in all considered cases, and the truncation error is less than 10^{-13}.

TABLE IV
REQUIRED TERMS N_4 FOR THE TRUNCATION ERROR ($\varepsilon_2<10^{-7}$) WITH DIFFERENT PARAMETERS a.

The non-linearity parameters	N_4	ε_2
$\alpha=4$	3	1.22543×10^{-8}
$\alpha=2$	4	4.5224×10^{-10}
$\alpha=1$	5	1.01573×10^{-11}

Table IV proves the convergence of the infinite series in (16) by presenting the required truncation terms N_4 for different parameters. Note that only less than 5 terms are needed for the series to converge in all considered cases, and the truncation error is less than 10^{-7}.

Remark 1. *The variable-gain AF relaying and DF relaying schemes have a similar performance because the end-to-end SNR of the variable-gain relaying system can be expressed as* $\gamma=\frac{\gamma_{RF}\gamma_{FSO}}{\gamma_{RF}+\gamma_{FSO}+1}\cong\min(\gamma_{RF},\gamma_{FSO})$ *[11]. The mathematical derivation of variable-gain AF relaying system is left for our future work.*

IV. PERFORMANCE ANALYSIS

A. Outage Probability

Mathematically speaking, the OP can be elucidated as the probability that the instantaneous end-to-end SNR falls below a particular outage threshold, γ_{th}, which is given as follows

$$P_{out}(\gamma_{\text{th}})=P_r[\gamma<\gamma_{\text{th}}]=F_{\gamma}(\gamma_{\text{th}}). \quad (24)$$

B. Average Bit-Error Rate

For a variety of binary modulation schemes, the average BER can be written in terms of the CDF of γ as [39]

$$\bar{P}_e=\frac{\delta}{2\Gamma(p)}\sum_{k=1}^{n}q_k^p\int_0^{\infty}\gamma^{p-1}\exp(-q_k\gamma)F_{\gamma}(\gamma)\,d\gamma, \quad (25)$$

where δ, n, p, q_k depend on the particular types of modulation schemes as well as heterodyne or IM/DD detection. The average BER for coherent binary phase shift keying (DBPSK) is given by (25) with $(\delta,n,p,q_k)=(1,1,1,1)$.

1) Fixed-Gain AF Relaying:

Theorem 1. *We can obtain the ABER of the considered system under the AF relay by substituting* (10) *into* (25)

$$\bar{P}_e^{AF}=\frac{n\delta}{2}-\frac{\delta B_1H_1}{2\Gamma(p)}\sum_{h=1}^{\beta}\sum_{k=0}^{\infty}\sum_{k_1=1}^{n}H_{2,2}^{2,1}\left[\frac{1}{2(1-\rho_{FSO}^2)q_k^2}\middle|\begin{matrix}(0,2)\,(1,1)\\(\frac{1+i}{2},1)\,(0,1)\end{matrix}\right]$$
$$+\frac{\delta B_1b_h\varphi_1C_2}{2\Gamma(p)}\sum_{h=1}^{\beta}\sum_{k=0}^{\infty}\sum_{i=0}^{\infty}\sum_{k_1=1}^{n}q_{k_1}^{-\frac{1+i}{r}}H_{1,0:1,3:1,2}^{0,1:2,1:1,1}$$
$$\left[\begin{matrix}\left(1+\frac{1+i}{r};1,\frac{2}{r}\right)\\-\\(1,1)\\(1,1)\,(\frac{1+k}{2},1)\,(0,1)\\(1,1)\\(\frac{1+i}{r}+p,\frac{2}{r})\,(\frac{1+i}{r},\frac{2}{r})\end{matrix}\middle|\,C_R\varphi,\left(\frac{q_{k_1}}{\psi_1}\right)^{\frac{2}{r}}\right]. \quad (26)$$

Proof: The average BER (26) can be written as (27) by representing $\exp(-q_{k_1}\gamma)$ as $H_{0,1}^{1,0}\left[q_k\gamma\middle|\begin{matrix}-\\0;1\end{matrix}\right]$, then using [40, Th.2.3] and [34, Eq (3.381/4)].

$$\bar{P}_e^{AF}=\frac{n\delta}{2}-B_1H_1\frac{\delta}{2\Gamma(p)}\sum_{h=1}^{\beta}\sum_{k=0}^{\infty}\sum_{k_1=1}^{n}q_{k_1}^p\int_0^{\infty}\gamma^{p-1}$$
$$\times H_{0,1}^{1,0}\left[q_k\gamma\middle|\begin{matrix}-\\(0,1)\end{matrix}\right]H_{1,2}^{2,0}\left[\frac{\gamma^2}{2(1-\rho_{\text{FSO}}^2)}\middle|\begin{matrix}1\\(\frac{1+i}{2},1)\,(0,1)\end{matrix}\right]d\gamma$$
$$+\frac{\delta}{2\Gamma(p)}\sum_{h=1}^{\beta}\sum_{k=0}^{\infty}\sum_{k_1=1}^{n}q_{k_1}^{-\frac{1+i}{r}}C_2B_1b_h\varphi_1$$
$$\times\left(\frac{1}{2\pi i}\right)^2\int_{L_1}\int_{L_2}\frac{\Gamma(1-s)\Gamma(s)\Gamma\left(\frac{1+k}{2}-s\right)}{\Gamma(1+s)}$$
$$\times\frac{\Gamma\left(s-\frac{1+i}{r}+\frac{2s_1}{r}\right)\Gamma(s_1)\Gamma\left(p+\frac{1+i}{r}-\frac{2s_1}{r}\right)}{\Gamma\left(1-\frac{1+i}{r}+\frac{2s_1}{r}\right)}(\varphi C_R)^s\left(\frac{q_{k_1}}{\psi_1}\right)^{\frac{2}{r}}dsds_1. \quad (27)$$

The proof is completed with the help of [37, Eq. (1.1)]. ■

$$\bar{P}_e^{DF} = \frac{n\delta(1-ZZ_1)}{2} + \frac{\delta ZC_2}{2\Gamma(p)} \sum_{k_1=1}^{n} \sum_{k=0}^{\infty} G_{2,2}^{1,2}\left[\frac{\varphi}{q_{k_1}}\middle|\begin{matrix}1-p,1\\ \frac{1+k}{2},0\end{matrix}\right] + \frac{\delta Z_1 B_1}{2\Gamma(p)} \sum_{k_1=1}^{n}\sum_{h=1}^{\beta}\sum_{i=0}^{\infty} H_1 \frac{r^{\frac{i}{2}} 2^{p-\frac{1}{2}}}{(2\pi)^{\frac{r}{2}}} G_{r+2,2r}^{r,r+2}\left[\frac{4\psi_1^r}{r^r q_{k_1}^2}\middle|\begin{matrix}\Delta(r,1),\Delta(2,1-p)\\ \Delta(r,\frac{1+i}{2}),\Delta(r,0)\end{matrix}\right]$$
$$- \frac{\delta B_1 C_2 H_1}{2\Gamma(p)} \sum_{h=1}^{\beta}\sum_{k=0}^{\infty}\sum_{i=0}^{\infty}\sum_{k_1=1}^{n} q_{k_1}^{-\frac{1+k}{r}} H_{1,0:1,2:1,2}^{0,1:1,1:1,1}\left[\begin{matrix}(1-p;1,\frac{2}{r})\\ -\\ (1,1)\\ (\frac{1+k}{2},1)\,(0,1)\\ (1,1)\\ (\frac{1+i}{r}+p,\frac{2}{r})\,(0,1)\end{matrix}\middle|\begin{matrix}\\ \\ \\ \frac{\varphi}{q_{k_1}},\frac{\psi_1}{(q_{k_1})^{\frac{2}{r}}}\\ \\ \\ \\ \end{matrix}\right]. \tag{28}$$

2) DF Relaying:

Theorem 2. *By substituting* (12) *into* (25)*, we can derive the closed-form expression of the average BER as* (28)*, shown at the top of the next page.*

Proof: By representing $\exp(-q_{k_1}\gamma)$ as $H_{0,1}^{1,0}\left[q_k\gamma\middle|\begin{matrix}-\\ 0;1\end{matrix}\right]$, the average BER can be rewritten as

$$\begin{aligned}\bar{P}_e^{DF} &= \tfrac{n\delta(1-Z_0Z_1)}{2} + \tfrac{\delta}{2\Gamma(p)} ZC_2 \sum_{h=1}^{\beta}\sum_{k=0}^{\infty}\sum_{k_1=1}^{n} q_{k_1}^p \\ &\times \int_0^\infty \gamma^{p-1} H_{0,1}^{1,0}\left[q_k\gamma\middle|\begin{matrix}-\\ (0,1)\end{matrix}\right] G_{1,2}^{1,1}\left[\varphi\gamma\middle|\begin{matrix}1\\ \frac{1+k}{2},0\end{matrix}\right] d\gamma \\ &+ \tfrac{\delta}{2\Gamma(p)} B_1 H_1 Z_1 \sum_{h=1}^{\beta}\sum_{k=0}^{\infty}\sum_{k_1=1}^{n} q_{k_1}^p \\ &\times \int_0^\infty \gamma^{p-1} H_{0,1}^{1,0}\left[q_k\gamma\middle|\begin{matrix}-\\ (0,1)\end{matrix}\right] G_{1,2}^{1,1}\left[\psi_1\gamma^{\frac{2}{r}}\middle|\begin{matrix}1\\ \frac{1+i}{2},0\end{matrix}\right] d\gamma \\ &- \tfrac{\delta}{2\Gamma(p)} C_2 B_1 H_1 \sum_{h=1}^{\beta}\sum_{k=0}^{\infty}\sum_{k_1=1}^{n} q_{k_1}^p \\ &\times \int_0^\infty \gamma^{p-1} H_{0,1}^{1,0}\left[q_k\gamma\middle|\begin{matrix}-\\ (0,1)\end{matrix}\right] G_{1,2}^{1,1}\left[\varphi\gamma\middle|\begin{matrix}1\\ \frac{1+k}{2},0\end{matrix}\right] G_{1,2}^{1,1}\left[\psi_1\gamma^{\frac{2}{r}}\middle|\begin{matrix}1\\ \frac{1+i}{2},0\end{matrix}\right] d\gamma.\end{aligned} \tag{29}$$

With the help of [34, Eq (7.813/1)], [41, Eq (21)], and [37, Eq (2.3)], the proof is completed. ■

C. Effective Capacity

By definition, the effective capacity is given by

$$\begin{aligned}R &\triangleq -\tfrac{1}{A}\log_2(\mathbb{E}\{1+\gamma\}^{-A}) \\ &= -\tfrac{1}{A}\log_2\left(1 - A\int_0^\infty (1+\gamma)^{-A-1} F_\gamma^C(\gamma) d\gamma\right),\end{aligned} \tag{30}$$

where $A \triangleq \theta TB/ln2$ with the block length T, asymptotic decay-rate of the buffer occupancy θ, and the system bandwidth B [42].

1) Fixed-Gain AF Relaying:

Theorem 3. *By substituting* (10) *into* (7)*, the closed-form expression of the effective capacity can be derived as*

$$\begin{aligned}R^{AF} &= -\tfrac{1}{A}\log_2[1 - AB_1H_1 \sum_{h=1}^{\beta}\sum_{k=0}^{\infty} H_{2,3}^{3,1}\left[\frac{1}{2(1-\rho_{\text{FSO}}^2)}\middle|\begin{matrix}(0,2)\,(1,1)\\ (\frac{1+i}{2},1)(0,1)(4,2)\end{matrix}\right] \\ &+ \tfrac{1}{\Gamma(1+A)} B_1 \sum_{\mathrm{h}=1}^{\beta}\sum_{k=0}^{\infty}\sum_{i=0}^{\infty} b_h\varphi_1 C_2 \\ &H_{1,0:1,3:2,3}^{0,1:2,1:1,2}\left[\begin{matrix}(1+\frac{1+i}{r};1,\frac{2}{r})\\ -\\ (1,1)\\ (1,1)\,(\frac{1+k}{2},1)\,(0,1)\\ (1-A+\frac{1+i}{2},\frac{2}{r})\,(1,1)\\ (1+\frac{1+i}{r},\frac{2}{r})\,(\frac{1+i}{r},\frac{2}{r})\end{matrix}\middle|\varphi C_R, \left(\tfrac{1}{\psi_1}\right)^{\frac{2}{r}}\right]].\end{aligned} \tag{31}$$

Proof: By substituting (10) into (7), with the help of the definition of the bivariate Fox's H-functions, (31) can be rewritten as

$$\begin{aligned}R^{AF} &= -\tfrac{1}{A}\log[1 - A\int_0^\infty (1+\gamma)^{-A-1} B_1H_1 G_{1,2}^{2,0}\left[\frac{\gamma^2}{2(1-\rho_{\text{FSO}}^2)}\middle|\begin{matrix}1\\ \frac{1+i}{2},0\end{matrix}\right] d\gamma \\ &+ \sum_{h=1}^{\beta}\sum_{i=0}^{\infty}\sum_{k=0}^{\infty} C_2B_1b_h\varphi_1 \int_0^\infty (1+\gamma)^{-A-1} \gamma^{\frac{1+i-2s_1}{r}} d\gamma \\ &\times \left(\tfrac{1}{2\pi i}\right)^2 \int_{L_1}\int_{L_2} \tfrac{\Gamma\left(s-\frac{1+i}{r}+\frac{2s_1}{r}\right)\Gamma(1-s)\Gamma\left(\frac{1+k}{2}-s\right)\Gamma(s)}{\Gamma(1+s)} \\ &\times \tfrac{\Gamma(s_1)}{\Gamma\left(1-\frac{1+i}{r}+\frac{2s_1}{r}\right)} (\varphi C_R)^s \left(\tfrac{1}{\psi_1}\right)^{\frac{2s_1}{r}} ds ds_1.\end{aligned} \tag{32}$$

Based on [37, Eq. (1.1)], with the help of [35, Eq.(2.8.4)] and [34, Eq.(3.194/3) , [Eq.(8.384/1)], the proof is completed. ■

2) DF Relaying:

Theorem 4. *With the help of* (13)*, we expand the effective capacity under the DF scheme in* (7) *as* (24)*, shown at the top of the next page.*

Proof: With the help of [43, Eq (8.2.3)], and [40, Eq. (1.43)], the effective capacity can be expressed as (25), shown at the top of the next page.

Employing [34, Eq (7.811.5)], [41, Eq (21)], and [37, Eq (2.3)], (24) is deduced, thus completing the proof. ■

V. Numerical Results and Discussions

In this section, analytical results are presented to verify the effect of different system and channel parameters on the performance of the considered system. The Monte-Carlo simulation is provided to confirm the correctness of the derived results. We assume that, for different hop, the average SNR is the same in all figures.

$$R^{DF}=-\tfrac{1}{A}\log[1-ZZ_1+\tfrac{AZ}{\Gamma(1+A)}\sum_{k=0}^{\infty}C_2G_{2,3}^{2,2}\left[\varphi\middle|\begin{matrix}0,1\\A,\frac{1+k}{2},0\end{matrix}\right]+\tfrac{2^AAZ_1B_1H_1r^{\frac{i}{2}}}{(2\pi)^{\frac{r+1}{2}}}\sum_{\mathrm{h}=1}^{\beta}\sum_{i=0}^{\infty}G_{r+2,2r+2}^{r+2,r+2}\left[\tfrac{\psi_1^r}{r^r}\middle|\begin{matrix}\Delta(2,0)\Delta(r,1)\\\Delta(2,A)\Delta(r,\frac{1+i}{2}),\Delta(r,0)\end{matrix}\right]$$
$$-\tfrac{AB_1C_2H_12^Ar^{\frac{k}{2}}\Gamma(\frac{1+i}{2})}{(2\pi)^{\frac{r+1}{2}}}\sum_{\mathrm{h}=1}^{\beta}\sum_{i=0}^{\infty}G_{r+2,2r+2}^{r+2,r+2}\left[\tfrac{\psi_1^r}{r^r}\middle|\begin{matrix}\Delta(2,0),\Delta(r,1)\\\Delta(r,\frac{1+i}{2}),\Delta(r,0),\Delta(2,A)\end{matrix}\right]+\tfrac{A}{\varphi}H_1C_2B_1\sum_{\mathrm{h}=1}^{\beta}\sum_{k=0}^{\infty}\sum_{i=0}^{\infty}H_{1,2:1,1:2,2}^{2,0:1,1:1,2}\left[\begin{matrix}(-\frac{1+k}{r};1,\frac{2}{r})\,(0;1,\frac{2}{r})\\(-1;1,\frac{2}{r})\\(-A,1)\\(0,1)\\(1,1)\\(\frac{1+i}{2},1)\,(0,1)\end{matrix}\middle|\tfrac{1}{\varphi},\tfrac{\psi_1}{(\varphi)^{\frac{2}{r}}}\right] \tag{24}$$

$$\begin{aligned}R^{DF}=&-\tfrac{1}{A}\log[1-ZZ_1+AZ\textstyle\int_0^{\infty}(1+\gamma)^{-A-1}\sum_{i=0}^{\infty}C_2G_{1,2}^{1,1}\left[\varphi\gamma\middle|\begin{matrix}1\\\frac{1+k}{2},0\end{matrix}\right]d\gamma\\&+AZ_1B_1\textstyle\int_0^{\infty}(1+\gamma)^{-A-1}\sum_{h=1}^{\beta}\sum_{k=0}^{\infty}H_1G_{1,2}^{1,1}\left[\psi_1\gamma^{\frac{2}{r}}\middle|\begin{matrix}1\\\frac{1+i}{2},0\end{matrix}\right]d\gamma\\&-A\textstyle\int_0^{\infty}(1+\gamma)^{-A-1}\sum_{h=1}^{\beta}\sum_{i=0}^{\infty}\sum_{k=0}^{\infty}H_1C_2B_1G_{1,2}^{1,1}\left[\varphi\gamma\middle|\begin{matrix}1\\\frac{1+k}{2},0\end{matrix}\right]G_{1,2}^{1,1}\left[\psi_1\gamma^{\frac{2}{r}}\middle|\begin{matrix}1\\\frac{1+i}{2},0\end{matrix}\right]d\gamma].\end{aligned} \tag{25}$$

Fig. 2 is plotted for the outage probability calculated by (10) versus the average SNR $\bar{\gamma}=\bar{\gamma}_{\mathrm{RF}}=\bar{\gamma}_{\mathrm{FSO}}=10\ dB$, with $\rho_{\mathrm{RF}}=\rho_{\mathrm{FSO}}=0.5$, $N_{\mathrm{r}}=2$, $\alpha=2$, and $\mu=2$. For the FSO link, we have considered different values of a, β, and ξ under IM/DD detection technology, representing the severity level of atmospheric turbulence and pointing error impairments, respectively. The number of iterations of the Monte-Carlo simulation is 10^6. Due to the imperfect CSI, the OP performance decreases to an error floor. Additionally, Fig. 2 illustrates the influence of different atmospheric turbulence and pointing error impairments in the OP performance. As a and β decrease, which means more severe atmospheric turbulence, the error floor increases due to worse channel conditions. Obviously, the pointing error parameter ξ also has a significant influence on the OP performance. To this end, we can find out from this figure that the pointing error has a dominant influence on the OP performance compared to the atmospheric turbulence.

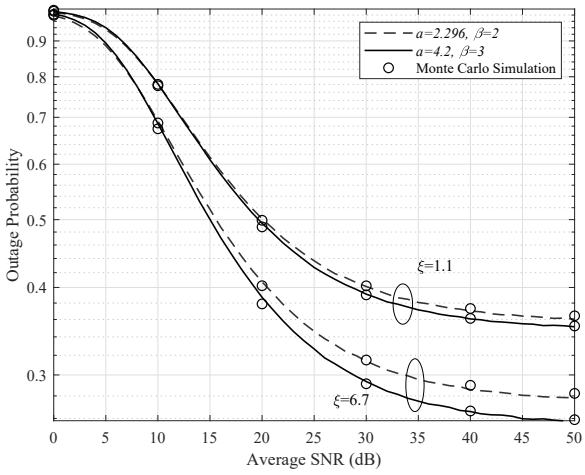

Fig. 2. Outage probability of dual-hop systems using AF relaying under IM/DD detection with imperfect CSI ($\rho_{RF}=\rho_{FSO}=0.5, N_r=2, \alpha=2, \mu=2$).

In Fig. 3, under various relaying schemes, we investigate the OP versus average SNR ($\bar{\gamma}$) under heterodyne detection with imperfect CSI. We set $\rho_{RF}=\rho_{FSO}=0.85, N_r=2, a=8, \beta=4$, and $\xi=6.7$. Fig. 3 describes the impact of the non-linearity of the environment (α) on the system performance. As expected, the larger the value of α, the lower the OP of the system. It is clear to observe that compared to the DF scheme, the fixed-gain AF relay has better performance for the same average SNR, which means a lower error floor. Notice that this is because AF relay has better performance than DF scheme at low SNR, and under the condition of imperfect CSI, the OP will reach an error floor when SNR is large enough. Under the fixed-gain AF relay, α has less influence on the system. In addition, the Monte-Carlo simulations also reveal the validity of our analysis. Moreover, we provided Monte-Carlo simulations for variable-gain AF relaying to provide the performance similarity comparison between variable gain AF relay and DF relay.

The OP performance of the considered system under negligible pointing error with imperfect CSI as a function of $\bar{\gamma}$ is illustrated in Fig. 4. Assuming $\rho_{\mathrm{RF}}=\rho_{\mathrm{FSO}}=0.9, N_{\mathrm{r}}=2, \alpha=2, \mu=2, and\ \xi=6.7$, we investigate the effect of different detection technologies and atmospheric turbulence on the OP performance. For high values of $\bar{\gamma}$, the asymptotic OP expressions (15) and (16) are also introduced. As can be seen from Fig. 4, the OP performance achieves an error floor due to the imperfect CSI, which eventually results in a zero diversity order at high SNRs. At moderate SNRs, the diversity order agrees with (18). The closed-form expressions are shown in (13), which coincide with the Monte-Carlo simulations. As expected, the highest OP is observed when the channel suffers light atmospheric turbulence and with heterodyne detection ($a=8, \beta=4$, and $r=1$). At the cost of a more complicated FSO receiver, the performance improvement of heterodyne detection techniques is acquired.

The impact of imperfect CSI at the OP performance of the

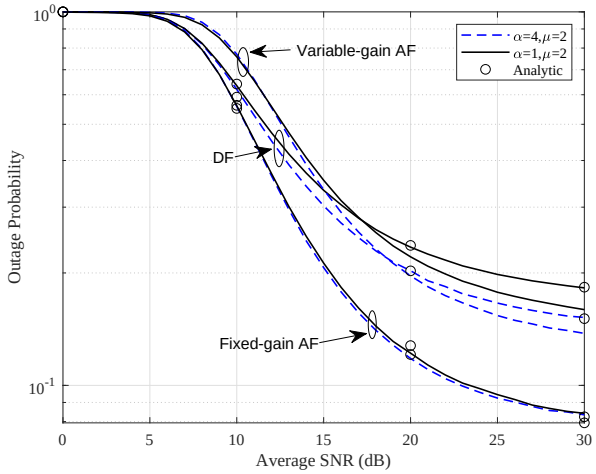

Fig. 3. Outage probability of dual-hop systems using variable-gain AF, fixed-gain AF, and DF relaying under heterodyne detection with imperfect CSI ($\rho_{RF} = \rho_{FSO} = 0.85, N_r = 2, a = 8, \beta = 4, \xi = 6.7$).

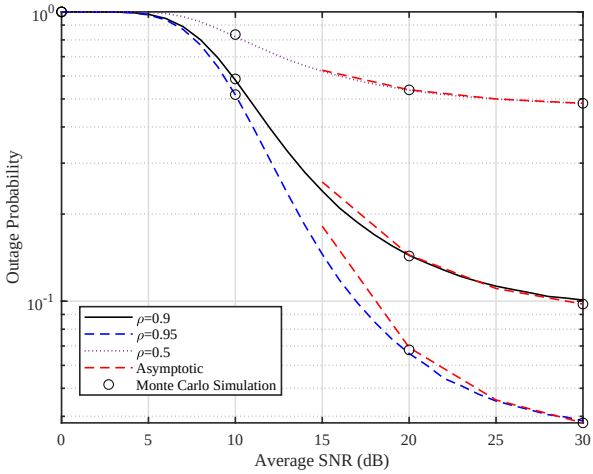

Fig. 5. Outage probability of dual-hop systems using DF relaying under heterodyne (r = 1) techniques with imperfect CSI ($a = 8, \beta = 4, N_r = 2, \alpha = 2, \mu = 2, \xi = 6.7$).

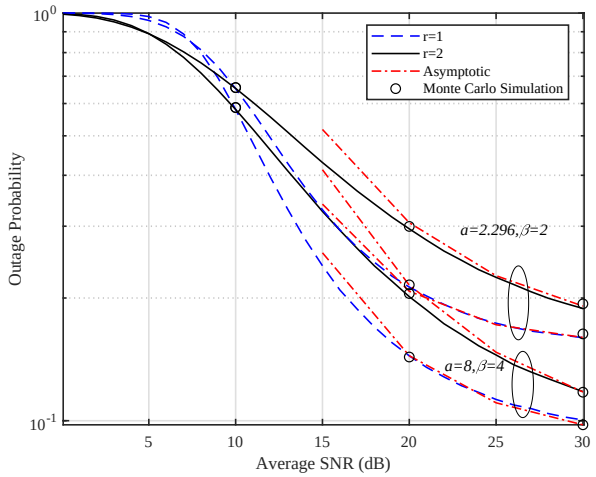

Fig. 4. Outage probability of dual-hop systems using DF relaying under IM/DD (r = 2) and heterodyne (r = 1) techniques with imperfect CSI ($\rho_{RF} = \rho_{FSO} = 0.9, N_r = 2, \alpha = 2, \mu = 2, \xi = 6.7$).

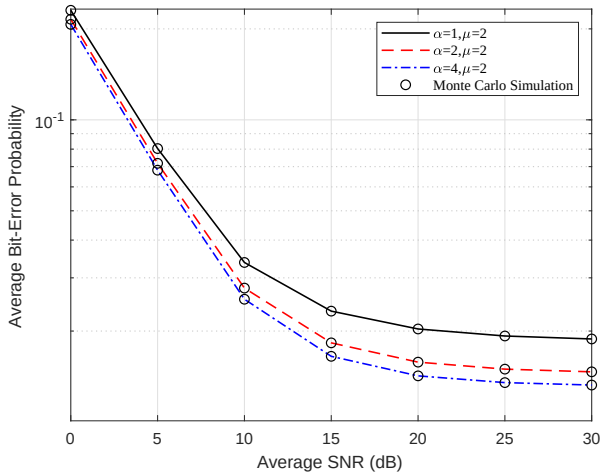

Fig. 6. Average bit error rate of dual-hop systems using DF relaying under heterodyne detection with imperfect CSI ($\rho_{RF} = \rho_{FSO} = 0.95, N_r = 4, a = 8, \beta = 4, \xi = 6.7$).

consider system assuming $a = 8, \beta = 4, N_r = 2, \alpha = 2, \mu = 2, \xi = 6.7$ is considered in Fig. 5. We investigate the various values of ρ, which mean the level of different imperfect CSI, to show clearly the impact of imperfect CSI on the system performance with respect to the perfect CSI scenario. The asymptotic results in (15) and (16) match the outage curves at high SNR values and the Monte-Carlo simulations also reveal the validity of our analysis.

Fig. 6 demonstrates the accurate formula for the BER in (19) of the mixed RF/FSO system with imperfect CSI through Monte-Carlo simulations. Under DF relaying, the DBPSK modulation scheme is employed over light atmospheric turbulence conditions ($a = 8, \beta = 4$) and negligible pointing error ($\xi = 6.7$) to investigate the BER performance of the system. Operating heterodyne detection, we studied the effect of the non-linearity of the environment (α). We also observe that due to imperfect CSI, the performance of BER converges to an error floor. As it is evident, the BER reduces when the value of α increases and vice versa.

In Fig. 7, we investigate the effective capacity versus average SNR ($\bar{\gamma}$) under heterodyne detection with imperfect CSI. Consistent with Fig. 5, we set $\rho_{\mathrm{RF}} = \rho_{\mathrm{FSO}} = 0.95, N_{\mathrm{r}} = 4, a = 8, \beta = 4$, and $\xi = 6.7$. For the SIMO RF links, as expected, it is easy to observe the effect of the number of multipath clusters (μ). As expected, the higher is the value of μ, the larger is the effective capacity of the considered system. Also, one can observe that the gap of the relevant curves narrows, which means that the parameter μ has a less significant effect on the effective capacity performance. Finally, for SNR grater than $\bar{\gamma} = 30$ dB, a performance upper

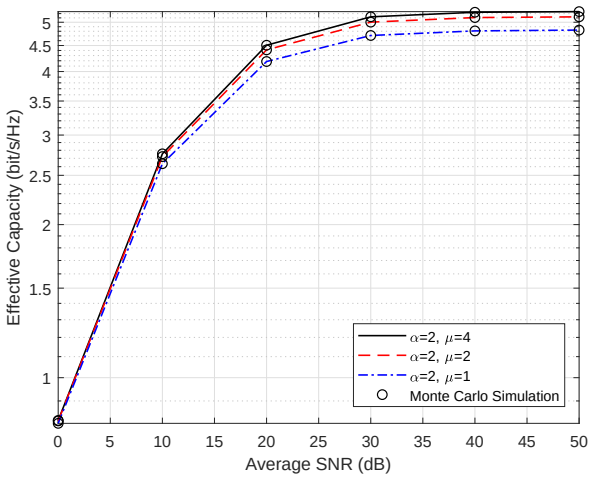

Fig. 7. Effective capacity of dual-hop systems using DF relaying under heterodyne detection with imperfect CSI ($\rho_{RF} = \rho_{FSO} = 0.95, N_r = 4, a = 8, \beta = 4, \xi = 6.7$).

bound takes place as expected from mathematical analysis in (24) due to the imperfect CSI.

VI. Conclusion

In this paper, we present novel closed-form performance results for the hybrid RF/FSO relaying system with imperfect CSI over $\alpha-\mu$ fading and Málaga ($\mathcal{M}$) channels, respectively. For the FSO link, we consider the effects of atmospheric turbulence with pointing errors. Utilizing IM/DD and heterodyne techniques, we derive exact closed-form expressions of the considered system, such as the outage probability, bit error probability, and effective capacity. Furthermore, we investigate the key effects of the link's correlation parameters, the channel estimation error, the number of antennas, the non-linearity of the environment, and the average SNRs on the system performance metrics. In addition, at high SNRs, we derive highly tight asymptotic results for the performance metrics.

Appendix A
Proof of Lemma 1

As is shown in [14, Eq. (18)-Eq. (25)], a single $\alpha-\mu$ RV $|h_{\mathrm{RF,s}}|^2$ with parameters $(\alpha, \mu, \hat{r})$ can be used to approximate the sum of N_{r} i.i.d. $\alpha-\mu$ RVs $|h_{\mathrm{RF,i}}|^2$ with parameters $(\alpha_{\mathrm{i}}, \mu_{\mathrm{i}}, \hat{r}_{\mathrm{i}})$, and this approximation appears to reach precise results. The PDF of $h_{\mathrm{RF,s}}$ is given by [30]

$$f_{\mathrm{h_{RF,s}}}(x) \approx \frac{\alpha\mu^{\mu}x^{\alpha\mu-1}}{\hat{r}^{\alpha\mu}\Gamma(\mu)} \exp\left(-\mu\frac{x^{\alpha}}{\hat{r}^{\alpha}}\right). \tag{A.1}$$

In addition, the parameters α, μ, and $\hat{r}$ can be obtained by solving the following nonlinear equations.

$$\frac{\Gamma^2(\mu+2/\alpha)}{\Gamma(\mu)\Gamma(\mu+4/\alpha)-\Gamma^2(\mu+2/\alpha)} = \frac{E^2\left(\mathrm{h}^2_{\mathrm{RF,s}}\right)}{E\left(\mathrm{h}^4_{\mathrm{RF,s}}\right)-E^2\left(\mathrm{h}^2_{\mathrm{RF,s}}\right)},$$

$$\frac{\Gamma^2(\mu+4/\alpha)}{\Gamma(\mu)\Gamma(\mu+8/\alpha)-\Gamma^2(\mu+4/\alpha)} = \frac{E^2\left(\mathrm{h}^4_{\mathrm{RF,s}}\right)}{E\left(\mathrm{h}^8_{\mathrm{RF,s}}\right)-E^2\left(\mathrm{h}^4_{\mathrm{RF,s}}\right)},$$

$$\hat{r} = \left[\frac{\mu^{2/\alpha}\Gamma(\mu)E\left(\mathrm{h}^2_{\mathrm{RF,s}}\right)}{\Gamma(\mu+2/\alpha)}\right]^{\frac{1}{2}}. \tag{A.2}$$

Using the multinomial identity, the moments in (A.2) can be attained as [30, Eq. (25)]:

$$E\left(h^{2n}_{\mathrm{RF,s}}\right) = \sum_{n_1=0}^{n}\sum_{n_2=0}^{n_1}\cdots\sum_{n_{N_r-1}=0}^{n_{N_r-2}}\binom{n}{n_1}\binom{n_1}{n_2}\cdots\binom{n_{N_r-2}}{n_{N_r-1}} E\left(h^{2(n-n_1)}_{\mathrm{RF},1}\right)E\left(h^{2(n_1-n_2)}_{\mathrm{RF},2}\right)\cdots E\left(h^{2(n_{N_r}-1)}_{\mathrm{RF,N_r}}\right). \tag{A.3}$$

Due to the difficulty to obtain the analytical solution to the system of equations (A.2), we use the $fsolve$ function of Matlab. Setting $X = \rho_{\mathrm{RF}}h_{\mathrm{RF,s}}$, $Y = N_{\mathrm{r}}\sqrt{1-\rho^2_{\mathrm{RF}}}\varepsilon$, and $Z = \hat{h}_{\mathrm{RF,s}}$, the PDFs of X and Y can be expressed as

$$f_X(z) = \frac{\alpha\mu^{\mu}z^{\alpha\mu-1}}{\hat{r}^{\alpha\mu}\rho^{\alpha\mu}_{\mathrm{RF}}\Gamma(\mu)}\exp\left(-\frac{\mu z^{\alpha}}{(\hat{r}\rho_{\mathrm{RF}})^{\alpha}}\right), \tag{A.4}$$

$$f_Y(y) = \frac{1}{N_r\sqrt{2\pi(1-\rho^2_{\mathrm{RF}})}}e^{-\frac{y^2}{2N_r^2(1-\rho^2_{\mathrm{RF}})}}. \tag{A.5}$$

Based on the convolution theorem, the PDF of $Z = X + Y$ can be deduced as

$$\begin{aligned} f_Z(z) &= \int_0^{\infty} f_X(x)f_Y(z-x)dx \\ &= \frac{\alpha\mu^{\mu}}{N_{\mathrm{r}}\sqrt{2\pi(1-\rho^2_{\mathrm{RF}})}\hat{r}^{\alpha\mu}\rho^{\alpha\mu}_{\mathrm{RF}}\Gamma(\mu)}\kappa(z), \end{aligned} \tag{A.6}$$

where

$$\kappa(z) = \int_0^{\infty} x^{\alpha\mu-1}\exp\left[-\frac{\mu x^{\alpha}}{(\hat{r}\rho_{\mathrm{RF}})^{\alpha}}\right]\exp\left[-\frac{(z-x)^2}{2N_r^2(1-\rho^2_{\mathrm{RF}})}\right]dx.$$

With the help of (11) and (21) in [41], then using [34, Eq. (9.31.5)] and $e^x = \sum_{k=0}^{\infty}\frac{x^k}{k!}$, we can get

$$\kappa(z) = \sum_{k=0}^{\infty}\frac{z^k 2^{\frac{k+\alpha\mu}{2}-1}(1-\rho^2_{\mathrm{RF}})^{\frac{\alpha\mu-k}{2}}(N_r)^{\frac{\alpha\mu-k+1}{2}}}{k!}\exp\left[-\frac{z^2}{2N_r^2(1-\rho^2_{\mathrm{RF}})}\right] \times H^{1,1}_{1,1}\left[\frac{\mu(2(N_r^2(1-\rho^2_{\mathrm{RF}})^2))^{\frac{\alpha}{2}}}{(\hat{r}\rho_{\mathrm{RF}})^{\alpha}}\middle|\begin{matrix}(1-\frac{\alpha\mu+k}{2},\frac{\alpha}{2})\\(0,1)\end{matrix}\right].$$

It is worth noting that, in practical models, the RF link's channel gain is positive. Hence, $f_{\hat{h}_{\mathrm{RF,s}}}(x)$ can be rewritten as

$$f_{\hat{h}_{\mathrm{RF,s}}}(z) = \begin{cases} \frac{\alpha\mu^{\mu}}{N_r\sqrt{2\pi(1-\rho^2_{\mathrm{RF}})}\hat{r}^{\alpha\mu}\rho^{\alpha\mu}_{\mathrm{RF}}\Gamma(\mu)}\kappa(z), & z>0 \\ 1-Z_1, & z=0 \end{cases} \tag{A.7}$$

Based on $\int_0^{\infty}h_{\mathrm{RF,s}}(z)dz = 1$ and [34, Eq. (3.326.2)], Z_1 can be obtained as

$$Z_1 = \sum_{k=0}^{\infty}\frac{\alpha 2^{\frac{k-3}{2}}H^{1,1}_{1,1}\left[\frac{\mu(2(1-\rho^2_{\mathrm{RF}})N_r^2)^{\frac{\alpha}{2}}}{(\rho_{\mathrm{RF}}\hat{r})^{\alpha}}\middle|\begin{matrix}(1-\frac{k}{2},\frac{a}{2})\\(\mu,1)\end{matrix}\right]}{k!\sqrt{\pi}\Gamma(\mu)N_r^{k+1}(1-\rho^2_{\mathrm{RF}})^{\frac{1+k}{2}}} \times\int_0^{\infty}z^k\exp\left[-\frac{z^2}{2N_r^{k+1}}\right]dz. \tag{A.8}$$

Using [34, Eq. (3.326.2)], (A.8) can be rewritten as

$$Z_1=\sum_{k=0}^{\infty}\frac{\alpha 2^{k-2}\Gamma(\frac{1+k}{2})H_{1,1}^{1,1}\left[\frac{\mu(2(1-\rho_{\rm RF}^2)N_t^2)^{\frac{\alpha}{2}}}{(\rho_{\rm RF}\hat{r})^{\alpha}}\middle|\begin{matrix}(1-\frac{k}{2},\frac{\alpha}{2})\\(\mu,1)\end{matrix}\right]}{k!\sqrt{\pi}\Gamma(\mu)}.$$

Utilizing [44, (07.34.21.0084.01)], the CDF of $\hat{h}_{\rm RF,s}$ can be expressed as

$$F_{\hat{h}_{\rm RF,s}}(z)=\begin{cases}\sum\limits_{k=0}^{\infty}\frac{\alpha\mu^{\mu}2^{\frac{k+\alpha\mu-3}{2}}N_t^{\alpha\mu-k-1}(1-\rho_{\rm RF}^2)^{\frac{\alpha\mu-k-1}{2}}}{k!\hat{r}^{\alpha\mu}\rho^{\alpha\mu}\sqrt{\pi}\Gamma(\mu)}\\ \times H_{1,1}^{1,1}\left[\frac{\mu(2(1-\rho_{\rm RF}^2)N_t^2)^{\frac{\alpha}{2}}}{(\rho_{\rm RF}\hat{r})^{\alpha}}\middle|\begin{matrix}(1-\frac{\alpha\mu+k}{2},\frac{\alpha}{2})\\(0,1)\end{matrix}\right], & z>0\\ 1-Z_1, & z=0\end{cases}$$

APPENDIX B
PROOF OF PROPOSITION 1

The CDF of the end-to-end SNR γ_{AF} can be written as

$$F_{\gamma_{AF}}(\gamma)=1-\int_{\gamma}^{\infty}f_{\hat{\gamma}_{\rm FSO}}(t)\,dt+\int_{0}^{\infty}f_{\hat{\gamma}_{\rm FSO}}(\gamma_1+\gamma)F_{\hat{\gamma}_{\rm RF}}(\frac{C_R\gamma}{\gamma_1})d\gamma_1. \tag{B.1}$$

Substituting (7) and (6) in (B.1), with the help of [34, Eq. (3.194/3), Eq. (8.384/1)] and [34, Eq. (3.381/9.*)], then based on the primary definition of the Meijer's G-function in [34, Eq. (9.301)], we deduced

$$\begin{aligned}F_{\gamma_{AF}}(\gamma)&=1-\int_{\gamma}^{\infty}B_1\sum_{h=1}^{\beta}\sum_{i=0}^{\infty}b_h\varphi_1 t^{\frac{i+1}{r}-1}e^{-\psi_1 t^{\frac{2}{r}}}dt\\&+\left(\tfrac{1}{2\pi i}\right)^2\int_{L_1}\int_{L_2}\frac{\Gamma\left(s-\frac{1+i}{r}+\frac{2s_1}{r}\right)\Gamma(1-s)\Gamma\left(\frac{1+k}{2}-s\right)\Gamma(s)}{\Gamma(1+s)}\\&\times\frac{\Gamma(s_1)}{\Gamma\left(1-\frac{1+i}{r}+\frac{2s_1}{r}\right)}(\varphi C_R)^s\left(\frac{1}{\psi_1\gamma}\right)^{\frac{2s_1}{r}}dsds_1\end{aligned}$$

where the contour L_1 and L_2 run from $-i\infty$ to $+i\infty$ with loops, in the s-plane and the t-plane, respectively. By employing [37, Eq. (1.1)], the CDF in (10) is deduced. Hence, the proof is completed.

REFERENCES

[1] M. J. Saber and S. Rajabi, "On secrecy performance of Millimeter-Wave RF-Assisted FSO Communication Systems," *IEEE Syst. J.*, May 2021.

[2] J. Zhang, E. Björnson, M. Matthaiou, D. W. K. Ng, H. Yang, and D. J. Love, "Prospective multiple antenna technologies for beyond 5G," *IEEE J. Sel. Areas Commun.*, vol. 38, no. 8, pp. 1637–1660, Aug. 2020.

[3] Q. Huang, M. Lin, W.-P. Zhu, J. Cheng, and M.-S. Alouini, "Uplink massive access in mixed RF/FSO satellite-aerial-terrestrial networks," *IEEE Trans. Commun.*, vol. 69, no. 4, pp. 2413–2426, Jan. 2021.

[4] H. Kaushal and G. Kaddoum, "Optical communication in space: Challenges and mitigation techniques," *IEEE Commun. Surveys Tuts.*, vol. 19, no. 1, pp. 57–96, Aug. 2016.

[5] Y. Zhang, J. Zhang, L. Yang, B. Ai, and M.-S. Alouini, "On the Performance of Dual-Hop Systems over Mixed FSO/mmWave Fading Channels," *IEEE Open J. Commun. Soc.*, vol. 1, pp. 477–489, May 2020.

[6] J. Zhang, J. Zhang, D. W. K. Ng, S. Jin, and B. Ai, "Improving sum-rate of Cell-Free massive MIMO with expanded compute-and-forward," *IEEE Trans. Signal Process.*, pp. 1–1, Nov. 2021.

[7] E. Lee, J. Park, D. Han, and G. Yoon, "Performance analysis of the asymmetric dual-hop relay transmission with mixed RF/FSO links," *IEEE Photon. Technol. Lett.*, vol. 23, no. 21, pp. 1642–1644, Nov. 2011.

[8] E. Soleimani-Nasab and M. Uysal, "Generalized performance analysis of mixed RF/FSO cooperative systems," *IEEE Trans. Wirel. Commun.*, vol. 15, no. 1, pp. 714–727, Jan. 2016.

[9] B. Ashrafzadeh, E. Soleimani-Nasab, M. Kamandar, and M. Uysal, "A framework on the performance analysis of dual-hop mixed FSO-RF cooperative systems," *IEEE Trans. Wireless Commun.*, vol. 67, no. 7, pp. 4939–4954, Jul. 2019.

[10] J. Zhang, L. Dai, Y. Zhang, and Z. Wang, "Unified performance analysis of mixed radio frequency/free-space optical dual-hop transmission systems," *IEEE/OSA J. Lightw. Technol.*, vol. 33, no. 11, pp. 2286–2293, Mar. 2015.

[11] E. Zedini, I. S. Ansari, and M.-S. Alouini, "Performance analysis of mixed Nakagami-m and Gamma–Gamma dual-hop FSO transmission systems," *IEEE Photon. J.*, vol. 7, no. 1, pp. 1–20, Feb. 2015.

[12] E. Zedini, H. Soury, and M.-S. Alouini, "On the performance analysis of dual-hop mixed FSO/RF systems," *IEEE Trans. Wireless Commun.*, vol. 15, no. 5, pp. 3679–3689, May 2016.

[13] H. Samimi and M. Uysal, "End-to-end performance of mixed RF/FSO transmission systems," *IEEE/OSA J. Opt. Commun. Netw*, vol. 5, no. 11, pp. 1139–1144, Nov. 2013.

[14] S. Li, L. Yang, D. B. da Costa, J. Zhang, and M.-S. Alouini, "Performance analysis of mixed RF-UWOC dual-hop transmission systems," *IEEE Trans. Veh. Technol.*, vol. 69, no. 11, pp. 14 043–14 048, Nov. 2020.

[15] Z. Jing, Z. Shang-hong, Z. Wei-hu, and C. Ke-fan, "Performance analysis for mixed FSO/RF Nakagami-m and Exponentiated Weibull dual-hop airborne systems," *Opt. Commun.*, vol. 392, pp. 294–299, Jun. 2017.

[16] B. Bag, A. Das, C. Bose, and A. Chandra, "Improving the performance of a DF relay-aided FSO system with an additional source–relay mmwave RF backup," *J. Opt. Commun. Netw.*, vol. 12, no. 12, pp. 390–402, Dec. 2020.

[17] I. Trigui, N. Cherif, and S. Affes, "Relay-assisted mixed FSO/RF systems over Málaga ($\mathcal{M}$) and $\kappa-\mu$ shadowed fading channels," *IEEE Wireless Commun. Lett.*, no. 99, pp. 1–1, 2017.

[18] B. Bag, A. Das, I. S. Ansari, A. Prokeš, C. Bose, and A. Chandra, "Performance analysis of hybrid FSO systems using FSO/RF-FSO link adaptation," *IEEE Photon. J.*, vol. 10, no. 3, pp. 1–17, May 2018.

[19] Y. Zhang, J. Zhang, K. P. Peppas, and B. Ai, "Performance analysis of dual-hop UAV relaying systems over mixed fluctuating Two-Ray and Nakagami-m fading channels," *Sci. China Inf. Sci.*, vol. 64, no. 4, pp. 1–3, Feb. 2021.

[20] S. Chen, J. Zhang, E. Björnson, J. Zhang, and B. Ai, "Structured massive access for scalable Cell-Free massive MIMO systems," *IEEE J. Sel. Areas Commun.*, vol. 39, no. 4, pp. 1086–1100, Apr. 2020.

[21] L. Yang, F. Meng, J. Zhang, M. O. Hasna, and M. D. Renzo, "On the performance of RIS-assisted dual-hop UAV communication systems," *IEEE Trans. Veh. Technol.*, Sept. 2020.

[22] N. Varshney and P. Puri, "Performance analysis of decode-and-forward-based mixed MIMO-RF/FSO cooperative systems with source mobility and imperfect CSI," *IEEE/OSA J. Lightw. Technol.*, vol. 35, no. 11, pp. 2070–2077, Jun. 2017.

[23] A. M. Salhab, "Performance of multiuser mixed RF/FSO relay networks with generalized order user scheduling and outdated channel information," *Arabian J. for Sci.*, vol. 40, no. 9, pp. 2671–2683, Sep. 2015.

[24] J. Zhang, L. Dai, Z. Wang, D. W. K. Ng, and W. H. Gerstacker, "Effective rate analysis of MISO systems over α-μ fading channels," in *Proc. IEEE Globecom.*, Dec. 2015, pp. 1–6.

[25] J. Zhang, H. Du, Q. Sun, B. Ai, and D. W. K. Ng, "Physical layer security enhancement with reconfigurable intelligent surface-aided networks," *IEEE Trans. Inf. Forensic Secur.*, vol. 16, pp. 3480–3495, May 2021.

[26] R. Boluda-Ruiz, A. García-Zambrana, B. Castillo-Vázquez, and C. Castillo-Vázquez, "Impact of nonzero boresight pointing error on ergodic capacity of MIMO FSO communication systems," *Opt. Express*, vol. 24, no. 4, pp. 3513–3534, Feb. 2016.

[27] H. Ran, J. Zhang, G. Pan, and Y. Xie, "Outage probability of wireless-powered Multi-relaying MIMO FSO-RF systems," *Opt. Commun.*, vol. 498, p. 127260, Jun. 2021.

[28] G. Pan, H. Lei, Y. Deng, L. Fan, J. Yang, Y. Chen, and Z. Ding, "On secrecy performance of MISO SWIPT systems with TAS and imperfect CSI," *IEEE Trans. Commun.*, vol. 64, no. 9, pp. 3831–3843, Sept. 2016.

[29] H. Lei, H. Luo, K.-H. Park, Z. Ren, G. Pan, and M.-S. Alouini, "Secrecy outage analysis of mixed RF-FSO systems with channel imperfection," *IEEE Photon. J.*, vol. 10, no. 3, pp. 1–13, May 2018.

[30] D. B. Da Costa, M. D. Yacoub *et al.*, "Highly Accurate Closed-Form Approximations to the Sum of α-μVariates and Applications," *IEEE Trans. Wireless Commun.*, vol. 7, no. 9, pp. 3301–3306, Sep. 2008.

[31] I. S. Ansari, F. Yilmaz, and M.-S. Alouini, "Performance analysis of free-space optical links over Málaga ($\mathcal{M}$) turbulence channels with pointing errors," *IEEE Trans. Wireless Commun*, vol. 15, no. 1, pp. 91–102, Jan. 2015.

[32] N. S. Ferdinand, D. B. da Costa, and M. Latva-aho, "Effects of outdated CSI on the secrecy performance of MISO wiretap channels with transmit antenna selection," *IEEE Commun. Lett.*, vol. 17, no. 5, pp. 864–867, May 2013.

[33] J. Feng and X. Zhao, "Performance analysis of OOK-based FSO systems in Gamma–Gamma turbulence with imprecise channel models," *Opt. Commun.*, vol. 402, pp. 340–348, Nov. 2017.

[34] I. S. Gradshteyn and I. M. Ryzhik, *Table of integrals, series, and products*. Academic press, 2014.

[35] A. A. Kilbas, *H-transforms: Theory and Applications*. CRC Press, 2004.

[36] M. O. Hasna and M.-S. Alouini, "A performance study of dual-hop transmissions with fixed gain relays," *IEEE Trans. Wireless Commun.*, vol. 3, no. 6, pp. 1963–1968, Nov. 2004.

[37] P. Mittal and K. Gupta, "An integral involving generalized function of two variables," in *Proceedings of the Indian academy of sciences-section A*, vol. 75, no. 3. Springer, 1972, pp. 117–123.

[38] Z. Wang and G. B. Giannakis, "A simple and general parameterization quantifying performance in fading channels," *IEEE Trans. Commun*, vol. 51, no. 8, pp. 1389–1398, Aug. 2003.

[39] E. Zedini, H. Soury, and M.-S. Alouini, "Dual-hop FSO transmission systems over Gamma–Gamma turbulence with pointing errors," *IEEE Trans. Wireless Commun.*, vol. 16, no. 2, pp. 784–796, Feb. 2017.

[40] R. K. S. A. Mathai and H. J. Haubold, *The H-function: Theory and Applications*. New York, NY, USA: Springer, 2010.

[41] V. Adamchik and O. Marichev, "The algorithm for calculating integrals of hypergeometric type functions and its realization in REDUCE system," in *Proc. Int. Symp. Symbolic Algebr. Comput.*, 1990, pp. 212–224.

[42] J. Zhang, H. Du, P. Zhang, J. Cheng, and L. Yang, "Performance analysis of 5G mobile relay systems for high-speed trains," *IEEE J. Sel. Areas Commun.*, vol. 38, no. 12, pp. 2760–2772, Jun. 2020.

[43] F. W. Olver, D. W. Lozier, R. F. Boisvert, and C. W. Clark, *NIST handbook of mathematical functions hardback and CD-ROM*. Cambridge university press, 2010.

[44] The Wolfram Functions Site. Accessed: 2021. [Online]. Available:, http://functions.wolfram.com.